DOI: 10.1002/asia.200600403

A_xBA_x-Type Block–Graft Polymers with Soft Methacrylate Middle Segments and Hard Styrene Outer Grafts: Synthesis, Morphology, and Mechanical Properties

Yu Miura,[a] Takeshi Kaneko,[b] Kotaro Satoh,[a] Masami Kamigaito,*[a] Hiroshi Jinnai,*[b] and Yoshio Okamoto[c]

Abstract: Novel copolymers with controlled architectures can function as new building blocks for well-defined nanostructures on the basis of microphase separation, unlike conventional ABA triblock copolymers. A series of well-defined A_xBA_x-type block–graft copolymers consisting of soft middle segments (dodecyl methacrylate (DMA)) and hard outer graft chains (styrene (St)) were synthesized by ruthenium-catalyzed living radical block and graft polymerization. NMR spectroscopy and size-exclusion chromatography combined with multiangle laser light scattering confirmed the well-defined structure of the A_xBA_x block–graft copolymers with backbones and graft chains of controlled lengths. Transmission electron microscopy and transmission electron microtomography revealed a series of morphologies for the copolymers. Morphological changes were observed from PSt "honeycomb" cylinders to lamellae and poly(DMA) cylinders with increasing PSt-graft content, whereby the phase diagram was shifted significantly to lower volume fractions of the larger-number component (St) relative to those of the corresponding ABA triblock copolymers. More specifically, poly(DMA) cylinders were observed even before the St content reached 50 wt%. The A_xBA_x and ABA copolymers with 17–30 wt% of St exhibited characteristics of a thermoplastic elastomer with tensile strengths of 1–6 MPa and elongations at break of 70–300%. These mechanical properties can be related well to the microphase structures of the A_xBA_x and ABA copolymers.

Keywords: block copolymers · mechanical properties · nanostructures · polymerization · ruthenium

Introduction

Well-defined block copolymers consisting of immiscible segments can form self-assembled ordered nano- or mesoscopic structures depending on their composition, their molecular weight, and the sequence of the segments.[1] Such nanoordered structures have been applied to the fabrication of microelectronic, separation, and optoelectronic devices as templates or scaffolds and have contributed to recent developments in nanotechnology.[2] Another wide application of such block copolymers is as thermoplastic elastomers (TPEs), which are based on ABA triblock copolymers with glassy outer chains coupled to a rubbery central chain,[3] such as polystyrene-*b*-polybutadiene-*b*-polystyrene. The microphase structure of TPEs determines their mechanical properties. The construction of the molecular structures, including the selection of monomers, molecular weight, composition, and sequence of the blocks is very important for materials design because these parameters greatly affect the

[a] Y. Miura, Dr. K. Satoh, Prof. M. Kamigaito
Department of Applied Chemistry
Graduate School of Engineering, Nagoya University
Furo-cho, Chikusa-ku, Nagoya 464-8603 (Japan)
Fax: (+81) 52-789-5112
E-mail: kamigait@apchem.nagoya-u.ac.jp

[b] T. Kaneko, Prof. H. Jinnai
Department of Macromolecular Science and Engineering
Graduate School of Science and Engineering
Kyoto Institute of Technology
Matsugasaki, Sakyo-ku, Kyoto 606-8585 (Japan)
Fax: (+81) 75-724-7800
E-mail: hjinnai@kit.ac.jp

[c] Prof. Y. Okamoto
EcoTopia Science Institute
Nagoya University
Furo-cho, Chikusa-ku, Nagoya 464-8603 (Japan)

Supporting information for this article is available on the WWW under http://www.chemasianj.org or from the author.

morphology, mechanical properties, and other characteristics of the material.

The effects of the molecular parameters of block copolymers on their morphology have been studied extensively for such copolymers prepared mainly by the living anionic polymerization of hydrocarbon monomers,[4] such as styrenes and dienes, under stringent conditions. A range of microphase ordered structures, such as spheres, cylinders, lamellae, and bicontinuous structures, have been made. Further developments in living-anionic-polymerization techniques with coupling agents have enabled the synthesis of more-complex copolymers that contain a combination of block and graft structures, such as A–*g*–B_x,[5,6] A_xB,[7–9] and A_xBA_x.[10,11] The effects of branching on the morphology have been discussed for some A_2B, A_3B, and A_5B miktoarm copolymers and A_2BA_2 H-shaped copolymers. Although these studies indicated that the morphology and mechanical properties could be changed drastically or controlled purposefully by altering the molecular structure of the block or graft copolymers, the limitations in the monomers and the cumbersome synthetic procedures inherent to living anionic polymerization, including repetitive purification by fractionation and/or preparative size-exclusion chromatography (SEC), restricted the variety of accessible polymers and their practical applications.

Progress in living and controlled radical polymerization has expanded the range of polymers with controlled architectures, such as block, graft, and star polymers, that are accessible from a variety of monomers, including nonpolar, polar, and functionalized monomers.[12–17] These techniques have also been applied to the synthesis of more-complex polymers with combined architectures, such as A–*g*–B_x,[18–22] A_xB,[23,24] A_xAA_x,[25] and A_xBA_x.[26–29] Although a variety of these structurally complex polymers have become readily accessible by living radical polymerization, few comprehensive and detailed studies have been carried out on the relationship between their architecture and their morphology and mechanical properties.[28,29] Such studies might contribute greatly to the development of new polymeric materials for emerging nanotechnologies.

Recently, we succeeded relatively easily in the preparation of a series of all-methacrylate well-defined A_xBA_x-type block–graft copolymers consisting of soft middle segments (dodecyl methacrylate (DMA)) and hard outer graft chains (methyl methacrylate (MMA)) by ruthenium-catalyzed living radical polymerization.[30] We characterized the copolymers by NMR spectroscopy, SEC, multiangle laser light scattering (MALLS), differential scanning calorimetry (DSC), dynamic viscoelasticity, and transmission electron microscopy (TEM) and visualized a single molecule of the copolymers by atomic force microscopy (AFM). These studies revealed that the synthesis had been quite successful without any cumbersome synthetic procedures or purification by fractionation and preparative SEC, and that branching affected the morphologies to provide different properties from those of the corresponding ABA triblock copolymers. However, the morphological details could not be understood fully owing to the difficulty in differentiating or segregating poly(DMA) segments from poly(MMA) (PMMA), both of which contain alkyl ester moieties.

With the aim of developing such novel A_xBA_x block–graft copolymers for the construction of ordered periodic nanoscale morphologies as well as new TPEs, we prepared a new series of A_xBA_x-type polymers with soft middle poly(DMA) segments and hard outer polystyrene (PSt) grafts and focused on the analysis of the morphologies by TEM and transmission electron microtomography (TEMT).[31] These techniques enabled the direct observation of nanoscale morphologies in three dimensions,[32] and the mechanical properties of the polymers were compared with those of the corresponding ABA triblock polymers. Our synthetic method was based on the ruthenium-catalyzed living radical block copolymerization of DMA and 2-(trimethylsilyloxy)ethyl methacrylate (TMSHEMA), which was initiated by a bifunctional initiator, followed by the direct in situ replacement of the trimethylsilyl groups with units containing a C–Br bond to create a multifunctional macroinitiator I_xBI_x, and subsequent ruthenium-catalyzed "grafting-from" living radical polymerization of St (Scheme 1).

Abstract in Japanese:

ルテニウム錯体によるリビングラジカル重合を用いることで、ハードなポリスチレン鎖をグラフト鎖として両側にもち、ソフトなポリ（メタクリル酸 *n*-ドデシル）を内側にもつ新規 A_xBA_x 型ブロック-グラフト共重合体の合成が容易に可能となった。透過型電子顕微鏡および三次元電子顕微鏡観測により、このような構造の明確な A_xBA_x 型共重合体は規則的なミクロ相分離構造を形成すると共に、従来の ABA トリブロック共重合体とは異なった相図を示すことが明らかとなった。また、粘弾性や力学特性においても、トリブロック共重合体とは異なった性質を示し、ハードなグラフト鎖とソフトな主鎖から成る A_xBA_x 型共重合体の新規熱可塑性材料としての可能性が示された。

Results and Discussion

Synthesis of Methacrylate–Styrene-Based A_xBA_x Block–Graft Copolymers

Prior to the synthesis of the A_xBA_x block–graft copolymers, the macroinitiators I_xBI_x, which consist of DMA (B) and multi-initiating sites (I; number-average molecular weight: $M_n = 132{,}000$ (by MALLS); molecular-weight distribution (MWD): $M_w/M_n = 1.17$; initiating sites: $F = 10.9$), were prepared as reported previously.[30] The ruthenium-catalyzed living radical polymerization of styrene was then initiated by the macroinitiator in the presence of $[Ru(Ind)Cl(PPh_3)_2]$ (Ind = indenyl) and nBu_3N in toluene at 100 °C to form the A_xBA_x block–graft copolymers.

Figure 1 shows the SEC curves, M_n, and M_w/M_n of the copolymers obtained simply by the precipitation of the polymerization mixtures into methanol. As the graft polymerization proceeded, the SEC curves shifted toward higher molecular weights with retention of the unimodal and narrow

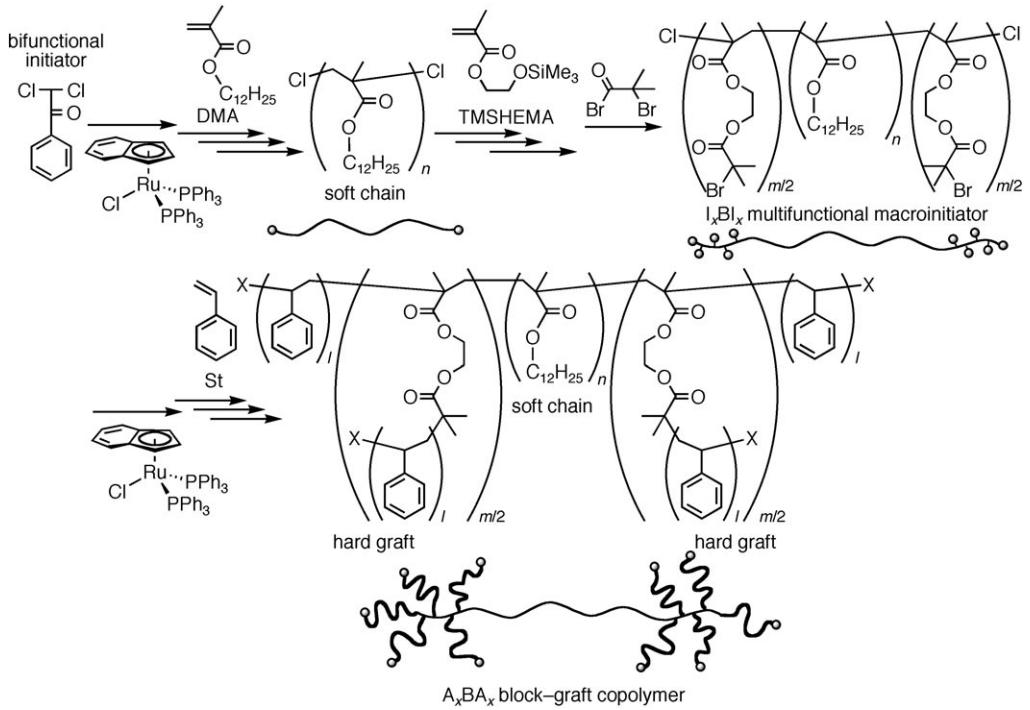

Scheme 1. Synthesis of A_xBA_x block–graft copolymers by ruthenium-catalyzed living radical polymerization.

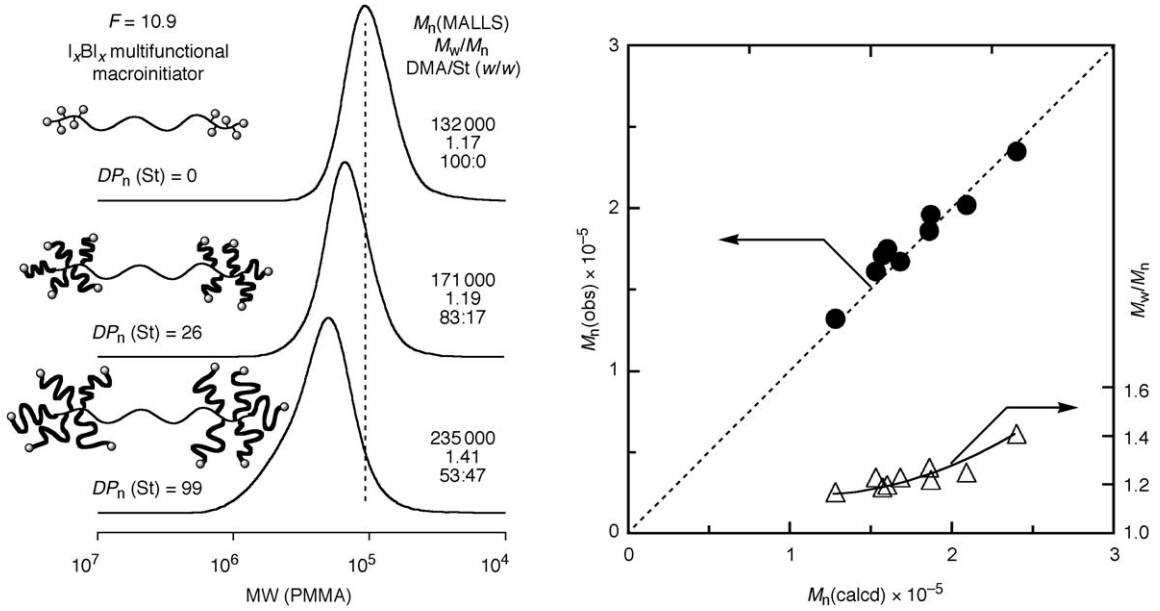

Figure 1. Graft polymerization of styrene (St) from the I_xBI_x multifunctional macroinitiator (M_n(MALLS) = 132000, M_w/M_n = 1.17) with [Ru(Ind)Cl-$(PPh_3)_2$]/nBu_3N in toluene at 80–100 °C. ● = M_n(MALLS), △ = M_w/M_n. $[St]_0$ = 3.0–6.0 M, initial concentration of C–X bonds in the macroinitiator = 10 mM, $[Ru(Ind)Cl(PPh_3)_2]_0$ = 1.0 mM, $[nBu_3N]_0$ = 5.0 mM.

MWDs ($M_w/M_n \leq 1.4$). The M_n values obtained by MALLS from the absolute molecular weights (M_w) agreed well with the calculated values if one assumes that one molecule of the I_xBI_x macroinitiator generates one molecule of the A_xBA_x polymer. However, the M_n values based on a PMMA standard calibration by SEC were lower than the calculated values owing to the smaller hydrodynamic volumes of the branched structures.[30] These results indicate the successful preparation of the methacrylate–styrene-based A_xBA_x copolymers by the ruthenium-catalyzed living radical grafting-from polymerization of styrene.

The A_xBA_x block–graft copolymers and the macroinitiators were also analyzed by ^1H NMR spectroscopy (Figure 2). The I_xBI_x macroinitiators (Figure 2a) showed the character-

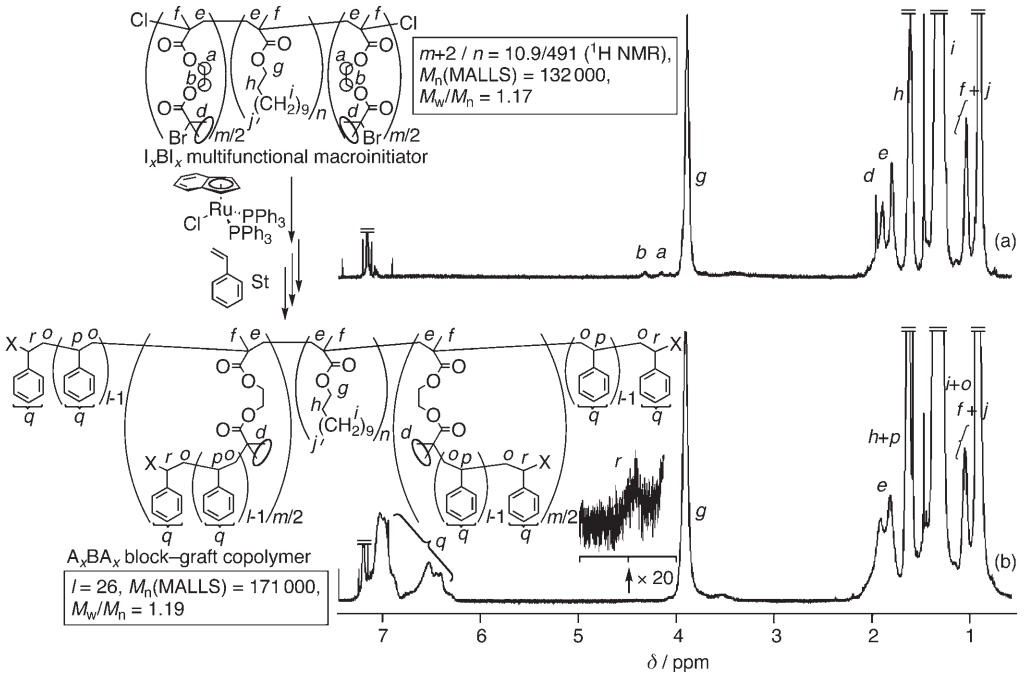

Figure 2. ^{1}H NMR spectra ($CDCl_3$, 50 °C) of a) the I_xBI_x multifunctional macroinitiator b) the A_xBA_x block–graft copolymer obtained with [Ru(Ind)Cl-$(PPh_3)_2$]/$n$$Bu_3N$ in toluene at 100 °C.

istic signals of DMA units, that is, those for the ester methylene hydrogen atoms (*g*) and the other hydrogen atoms of the alkyl chain (*h–j*), and of the multifunctional initiating sites, that is, those for the ester ethylene hydrogen atoms (*a*, *b*) and the methyl groups (*d*) adjacent to the C–Br bonds, as well as large absorptions for the α-methyl (*f*) and main-chain methylene hydrogen atoms (*e*) of both units. The unit ratio of DMA to the initiating sites as calculated from the peak-intensity ratio (*g* versus *b*) was 491:8.7, which agrees well with the calculated ratio of 491:8.9 for the macroinitiator. Thus, the macroinitiators obtained possessed about 11 initiating sites per molecule, including the C–Br bonds and the original C–Cl bonds at the chain ends.

The A_xBA_x block–graft copolymers showed the characteristic signals of the aromatic hydrogen atoms (*q*) of the polystyrene graft chains and the methine hydrogen atoms (*r*) adjacent to the C–X terminals, as well as the absorptions of the prepolymer (Figure 2b). The DMA/St unit ratio (83:17 *w*/*w*) calculated from the peak-intensity ratio (*g* versus *q*) agreed with the DMA/St ratio calculated from the monomer feed ratio and monomer conversion (81:19 *w*/*w*). These results also serve as evidence that the simple synthetic method based on ruthenium-catalyzed living radical block and graft polymerization is effective in the synthesis of the methacrylate–styrene A_xBA_x block–graft copolymers with controlled molecular weights and compositions. A series of the A_xBA_x block–graft polymers with varying graft-chain lengths were thus synthesized successfully by simply changing the monomer conversion, as summarized in Table 1. All of these copolymers had controlled molecular weights and narrow MWDs, and the monomer composition varied in the range DMA/St = 85:15–53:47 (*w*/*w*). Table 1 also shows that the molecular weight and mean radius of gyration (R_z) generally increased with the length (*l*) of the graft chains, although some exceptional cases were observed, probably as a result of experimental error in the measurements.

The polystyrene (PSt) graft chains in the A_xBA_x block–graft copolymers prepared in this way are connected to the backbone chain through ester linkages; the ester linkages of the backbone and the graft chains can be hydrolyzed. To confirm the molecular weights and uniformity of the PSt graft chains, the copolymers were hydrolyzed with potassium hydroxide in a mixture of methanol and *N*,*N*-dimethylformamide (1:3 *v*/*v*) at 80 °C (Scheme 2).[22]

Figure 3 shows a series of SEC curves of the hydrolyzed products (dashed and dotted lines) from the A_xBA_x block–graft copolymers obtained at different monomer conversions as well as that of the I_xBI_x macroinitiator (solid line). After the hydrolysis, each SEC curve had two peaks. The peak at higher molecular weight was attributed to the original backbone chain from which the PSt grafts were removed, whereas the peak at lower molecular weight was ascribed to the detached PSt graft chains. The peaks at lower molecular weight shifted with styrene conversion and showed narrow MWDs ($M_w/M_n < 1.4$). The M_n values of the detached PSt graft chains increased with monomer conversion (solid diagonal line). However, they were consistently slightly higher than the values calculated on the assumption that each initiating site generates one PSt graft chain (dashed diagonal line), probably because the initiation efficiency of the initiating units in the macroinitiator was slightly lower than unity. A similar result was also observed for copper-catalyzed graft polymerization for the synthesis of densely grafted copolymers.[35] These results indicate that most initiating sites ini-

Table 1. A_xBA_x block–graft and ABA triblock copolymers obtained by ruthenium-catalyzed living radical polymerization.[a]

Code	n[b]	F[b] (m+2)	I[b]	M_w[c] (MALLS)	M_n calcd[d]	M_n SEC[e]	M_n MALLS[f]	M_w/M_n[e]	R_z[c] [nm]	dn/dc[g] [mL g^{-1}]	DMA/St (w/w) calcd[h]	DMA/St (w/w) obs[b]	$f_{PSt,vol}$[i]	T_g[j] [°C]
1	491	10.9	0	154000	128000	97000	132000	1.17	22.9	0.0715	–	–	–	n.d.
2	491	10.9	22	198000	153000	115000	161000	1.23	25.3	0.0946	83:17	85:15	0.14	n.d.
3	491	10.9	26	203000	157000	114000	171000	1.19	25.4	0.0980	81:19	83:17	0.15	−50.8, 42.9
4	491	10.9	28	210000	160000	122000	175000	1.20	25.8	0.1036	80:20	82:18	0.16	n.d.
5	491	10.9	35	206000	168000	124000	167000	1.23	26.8	0.1080	76:24	77:23	0.21	−51.6, 54.1
6	491	10.9	51	236000	186000	142000	186000	1.27	28.8	0.1292	69:31	70:30	0.27	−51.1, 67.5
7	491	10.9	52	239000	187000	136000	196000	1.22	28.2	0.1261	68:32	70:30	0.27	n.d.
8	491	10.9	71	252000	209000	152000	202000	1.25	30.1	0.1376	60:40	62:38	0.35	−51.5, 73.2
9	491	10.9	99	332000	240000	197000	235000	1.41	33.8	0.1603	52:48	53:47	0.44	−52.2, 80.5
10	560	2	0	176000	142000	123000	149000	1.18	24.4	0.0825	–	–	–	n.d.
11	560	2	158	229000	175000	170000	191000	1.20	27.3	0.1120	81:19	81:19	0.17	−51.4, 86.1
12	560	2	298	273000	204000	214000	228000	1.20	30.5	0.1276	70:30	70:30	0.27	−51.0, 92.5

[a] Polymerization conditions: $[St]_0/[C{-}X$ bonds in the macroinitiator$]_0/[[Ru(Ind)Cl(PPh_3)_2]]_0/[n Bu_3N]_0 = 3000$–$6000{:}10{:}1.0{:}5.0$ mM in toluene at 80–100 °C (codes 1–9); $[St]_0/[C{-}X$ bonds in the macroinitiator$]_0/[[Ru(Cp^*)Cl(PPh_3)_2]]_0/[n Bu_3N]_0 = 2000{:}2.5{:}4.0{:}40$ mM in toluene at 80 °C (codes 10–12). Cp* = pentamethylcyclopentadienyl. [b] Determined by ^{1}H NMR spectroscopy. [c] Measured by SEC with a multiangle laser light scattering (MALLS) detector ($\lambda = 633$ nm). [d] M_n(calcd) = M_n(macroinitiator, calcd) + ([M]$_0$/[C−X]$_0$) × conversion × F × MW(St). [e] The number-average molecular weight (M_n), the weight-average molecular weight (M_w), and the polydispersity index (M_w/M_n) were determined by size-exclusion chromatography (SEC) with a refractive-index (RI) detector (PMMA standard). [f] M_n(MALLS) = M_w(MALLS)/(M_w/M_n(SEC)). [g] The refractive index increment was measured with a refractometer ($\lambda = 633$ nm). [h] Calculated from the feed ratio and monomer conversion. [i] Calculated from the reported densities: d(poly(DMA)) = 0.929 g cm^{-3},[33] d(PSt) = 1.05 g cm^{-3}.[34] [j] The glass transition temperature was determined by differential scanning calorimetry (DSC); n.d. = not determined.

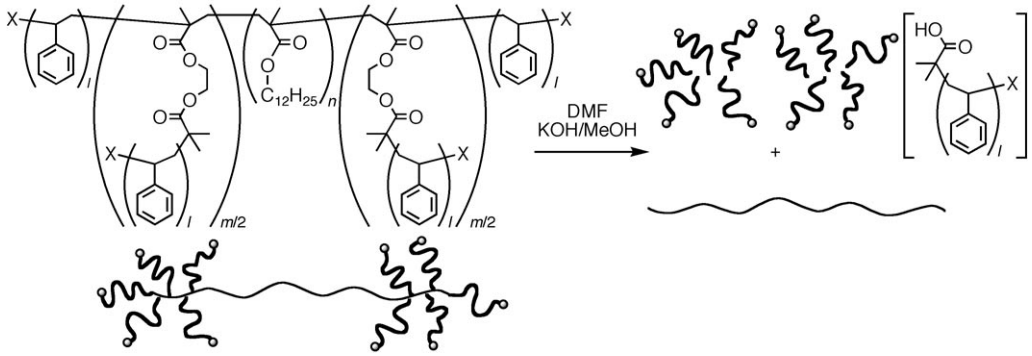

Scheme 2. Detachment of PSt graft chains from the backbone chain. DMF = *N*,*N*-dimethylformamide.

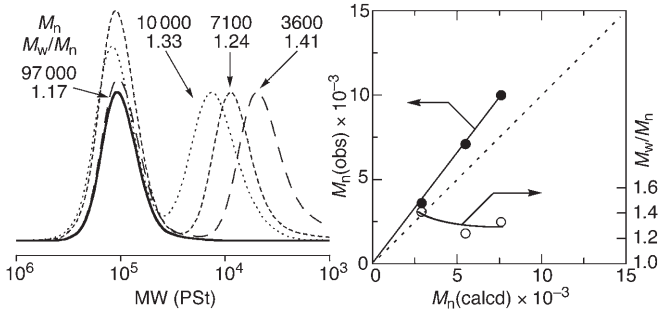

Figure 3. SEC curves of the original I_xBI_x multifunctional macroinitiator (solid line) and the hydrolyzed products from the A_xBA_x block–graft copolymers (codes 3, 6, and 8 in Table 1; dashed or dotted lines), and M_n (●) and M_w/M_n (○) of the detached PSt graft chains.

tiate the graft polymerization of styrene to form PSt graft chains with controlled molecular weights and produce well-defined methacrylate–styrene-based A_xBA_x block–graft copolymers.

Morphology of A_xBA_x Block–Graft Copolymers

We analyzed the bulk morphology of a series of the methacrylate–styrene-based A_xBA_x block–graft copolymers, the PSt-graft-chain lengths of which were changed systematically while keeping the molecular weight of the middle poly(DMA) segments the same. We found by TEM that the DMA/St content of these polymers varied in the range 85:15–53:47 (w/w) (Figure 4). In these TEM images, the PSt domains were stained dark with RuO_4. In contrast to the all-methacrylate A_xBA_x block–graft copolymers, which exhibited complex microphase-separated structures, probably as a result of the similarity in the structures of the PMMA and poly(DMA) segments,[30] the methacrylate–styrene-based counterparts were found to have clearer, nanoordered microphase-separated structures. As observed for the linear block polymers, the morphologies can be changed systematically by changing the composition. As the weight fraction of PSt ($f_{PSt,wt}$) increased, the morphology changed in the following order: spheres or cylinders of PSt ($f_{PSt,wt} = 0.15$ (Fig-

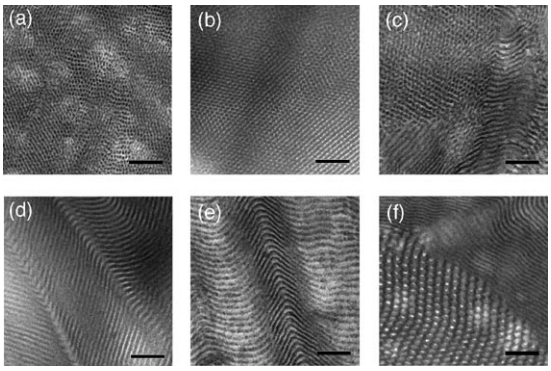

Figure 4. TEM images of the A_xBA_x block–graft copolymers ($F=10.9$). a) M_n(MALLS) = 161 000, $M_w/M_n=1.23$, B/A = 85:15; b) M_n(MALLS) = 171 000, $M_w/M_n=1.19$, B/A = 83:17; c) M_n(MALLS) = 167 000, $M_w/M_n=1.23$, B/A = 77:23; d) M_n(MALLS) = 186 000, $M_w/M_n=1.27$, B/A = 70:30; e) M_n(MALLS) = 202 000, $M_w/M_n=1.25$, B/A = 62:38; f) M_n(MALLS) = 235 000, $M_w/M_n=1.41$, B/A = 53:47. The films were stained with RuO_4; scale bars: 200 nm.

ure 4a)–0.17 (Figure 4b)), the coexistence of cylindrical and lamellar phases and/or cylindrical phases with different grains ($f_{PSt,wt}=0.23$ (Figure 4c)), lamellae ($f_{PSt,wt}=0.30$ (Figure 4d)–0.38 (Figure 4e)), and finally, the coexistence of poly(DMA) cylinders and lamellae or two cylindrical phases ($f_{PSt,wt}=0.47$ (Figure 4f)). Especially in the TEM image of the specimen with the 17 wt% PSt fraction (Figure 4b), a morphology of highly ordered, long-range hexagonally packed PSt domains in a poly(DMA) matrix was observed. More interestingly, the PSt cylinders appear to have a hexagon-like cross-section and thus form a "honeycomb" morphology, as described later. To make sure that these polymer morphologies can be observed over the entire samples, we also analyzed a series of the samples by TEM over a wider range (see the TEM images with lower magnification in the Supporting Information). These images showed similar morphologies to those in Figure 4 over the whole region.

Milner proposed that the introduction of a branched architecture into block copolymers results in asymmetry in the phase diagram: The larger excluded volume of the graft chains anchored around the domain boundary relative to that of a single block chain causes an interfacial curvature.[36] The volume-fraction windows for our A_xBA_x block–graft copolymers were thus shifted to lower volume fractions of the larger-number component (PSt in this case) than those for the corresponding linear block copolymers. These phenomena were also observed for A_2B, A_3B, and A_5B miktoarm copolymers and A_2BA_2 H-shaped copolymers of isoprene and styrene that were prepared by living anionic polymerization, although some deviations from the theory were suggested.[7–10] The A_xBA_x block–graft copolymers prepared by simple living radical polymerization also showed similar asymmetry to that predicted by Milner's theory and similar deviations from the theory. The coexistence of poly(DMA) cylinders and lamellae or two cylindrical phases vertical and parallel to the cross-sectional direction were observed even with a 47 wt% PSt fraction (Figure 4f). The microstructure was further clarified by TEMT, as described below. The possibility of controlling the morphology through the branching number without changing the volume fraction or the hardness of the material would be beneficial for materials design. Although it has already been shown for miktoarm and H-shaped polymers prepared by living anionic polymerizations that a particular morphological design can be attained not only by changing the volume fraction but also through changes in the molecular architecture, this study extends the concept to living radical polymerizations, which would be more practical for making materials.

To clarify the morphologies of the A_xBA_x block–graft copolymers in more detail, two samples were studied by TEMT: one with hexagon-like cylinder morphology ($f_{PSt,wt}=0.17$) and the other with mixtures of cylinders and lamellae or two cylindrical phases ($f_{PSt,wt}=0.47$). Figure 5 shows two-

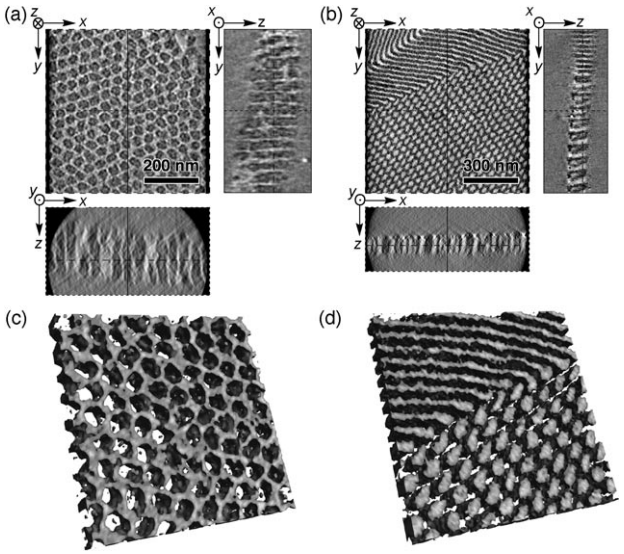

Figure 5. Two-dimensional planar (x, y) and cross-sectional (x, z; y, z) slices of the morphologies as observed by 3D TEMT (a and b) and 3D solid renditions of the poly(DMA) microdomains within a transparent PSt matrix (c and d: 400×400×50 nm). a, c) M_n(MALLS) = 171 000, $M_w/M_n=1.19$, B/A = 83:17; b, d) M_n(MALLS) = 235 000, $M_w/M_n=1.41$, B/A = 53:47). The z axis is parallel to the depth direction of the ultrathin section. Dashed and solid lines in each cross-section represent the position of two other orthogonal cross-sections.

dimensional planar (x, y) and cross-sectional (x, z; y, z) slices of the morphologies as observed by TEMT and 3D solid-rendered images of the poly(DMA) microdomains within a transparent PSt matrix. The electron beam comes from the z direction. The 3D reconstructed images of the morphologies in Figure 5c and d prove the existence of orthogonally aligned hexagon-like "honeycomb" cylinders ($f_{PSt,wt}=0.17$; Figure 5c), which are clearly different from normal circular cylinders, and the coexistence of lamellar/cylindrical morphologies ($f_{PSt,wt}=0.47$; Figure 5d), both of which are aligned with the z axis. Although the "honeycomb" morphology has been reported for multiple-component copolymers, such as ABC triblock, ABC heteroarm

star, and ABCD tetrablock copolymers and their blends, this is the first time that the hexagon-like "honeycomb" morphology has been observed in two-component A_xBA_x block–graft copolymers.[37–39] Furthermore, TEMT of the second sample ($f_{PSt,wt}=0.47$) indicated the coexistence of poly(DMA) cylinders and lamellae more clearly and directly.

To characterize further the morphologies built by the A_xBA_x block–graft copolymers in comparison to those of the ABA triblock copolymers, a series of PSt-*b*-poly(DMA)-*b*-PSt polymers with similar compositions were synthesized by ruthenium-catalyzed living radical polymerization according to Scheme 3. As summarized in Table 1, the triblock copolymers obtained also exhibited controlled molecular weights, narrow MWDs, and the desired compositions of DMA and St: Codes 11 and 12 of the ABA triblock copolymers have DMA/St ratios similar to those of codes 3, 4 and codes 6, 7 of the A_xBA_x block–graft copolymers, respectively.

The ABA samples with DMA/St = 81:19 (Figure 6a) and 70:30 (Figure 6b) exhibited spherical and cylindrical morphologies, respectively, as expected from the comonomer compositions for the conventional block copolymers. As mentioned above, the A_xBA_x samples with similar PSt compositions formed cylinders (Figure 6c; DMA/St = 83:17) and lamellae (Figure 6d; DMA/St = 70:30), respectively, in volume-fraction windows that were apparently shifted to lower volume fractions of the larger-number component. These morphologies were crucial for some of the mechanical properties observed. The A_xBA_x block–graft copolymers showed similar mechanical properties to ABA triblock copolymers with different compositions but similar morphologies.

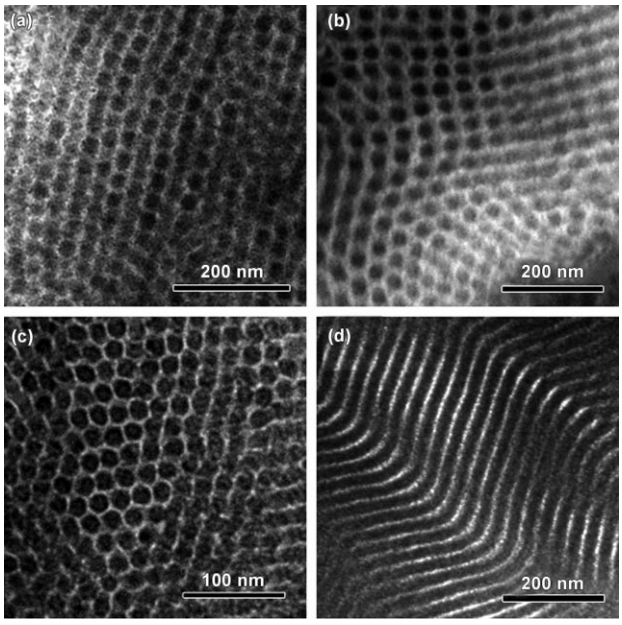

Figure 6. TEM images of the ABA triblock copolymers: a) M_n(MALLS) = 191000, $M_w/M_n=1.20$, B/A = 81:19; b) M_n(MALLS) = 228000, $M_w/M_n=1.20$, B/A = 70:30); and A_xBA_x block–graft copolymers ($F=10.9$): c) M_n(MALLS) = 171000, $M_w/M_n=1.19$, B/A = 83:17; d) M_n(SEC) = 186000, $M_w/M_n=1.27$, B/A = 70:30. The films were stained with RuO_4.

Mechanical Properties of A_xBA_x Block–Graft Copolymers

The mechanical characteristics of the A_xBA_x copolymers were evaluated in terms of their dynamic viscoelasticity and tensile stress–strain properties along with the ABA triblock copolymers. Figure 7 shows the dynamic tensile storage modulus (E') and tan δ ($=E''/E'$) as a function of temperature. In all spectra, the storage moduli showed the two loss peaks associated with the glass transitions of the poly(DMA) and PSt domains in the microphase-separated structure and a rubbery plateau between the two transition tem-

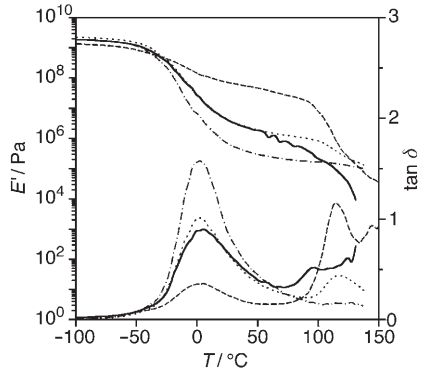

Figure 7. Dynamic tensile storage moduli (E') and tan δ as a function of temperature for the A_xBA_x block–graft copolymers ($F=10.9$; solid line: M_n(MALLS) = 175000, $M_w/M_n=1.20$, B/A = 82:18; dashed line: M_n(MALLS) = 196000, $M_w/M_n=1.22$, B/A = 70:30) and ABA triblock copolymers (dash-dotted line: M_n(MALLS) = 191000, $M_w/M_n=1.20$, B/A = 81:19; dotted line: M_n(MALLS) = 228000, $M_w/M_n=1.20$, B/A = 70:30). Heating rate: 10 °C min^{-1}; frequency: 11 Hz.

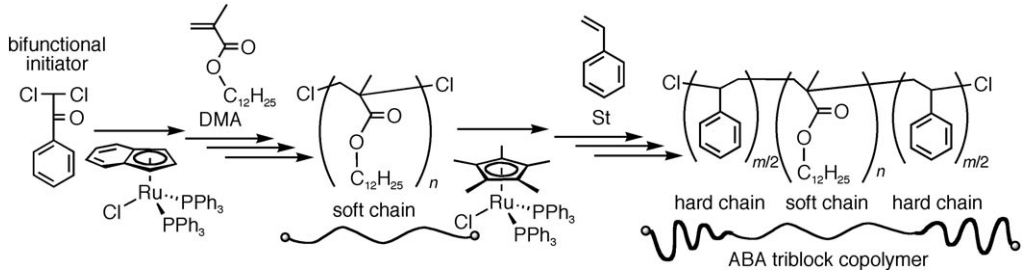

Scheme 3. Synthesis of ABA triblock copolymers by ruthenium-catalyzed living radical polymerization.

peratures. These results indicate that the A_xBA_x block–graft copolymers (dashed and solid lines) behave as thermoplastic elastomers between the two transitions, in which the PSt domains serve as anchor phases, in a similar way to the ABA triblock copolymers (dotted and dashed–dotted lines). The storage moduli of the plateau in the A_xBA_x block–graft copolymers were higher than those in the corresponding ABA triblock copolymers and became lower as the PSt content increased. More interestingly, at a lower temperature, the tensile moduli of A_xBA_x (solid line; code 4; DMA/St = 82:18) and ABA (dotted line; code 12; DMA/St = 70:30) were the same, although the polymers had different A/B compositions, and became different at a higher temperature as a result of the difference in the T_g values of the PSt segments. The differences in the morphologies probably led to the differences in these properties, as mentioned above.

Figure 8 shows the stress–strain curves of the A_xBA_x block–graft and ABA triblock copolymers. As also summarized in Table 2, the mechanical strength and strain at break

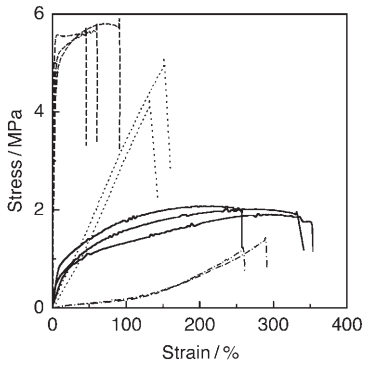

Figure 8. Stress–strain curves of the A_xBA_x block–graft copolymers (F = 10.9; solid line: M_n(MALLS) = 175 000, M_w/M_n = 1.20, B/A = 82:18, $f_{PSt,w}$ = 0.18; dashed line: M_n(MALLS) = 196 000, M_w/M_n = 1.22, B/A = 70:30, $f_{PSt,w}$ = 0.30) and ABA triblock copolymers (dash-dotted line: M_n(MALLS) = 191 000, M_w/M_n = 1.20, B/A = 81:19, $f_{PSt,w}$ = 0.19; dotted line: M_n(MALLS) = 228 000, M_w/M_n = 1.20, B/A = 70:30, $f_{PSt,w}$ = 0.30).

of all the copolymers were relatively low (1–6 MPa) compared to the values for commercially available styrene–diene block copolymers,[3] most probably as a result of the central poly(DMA) blocks, which have a high molecular weight between chain entanglements, M_e (M_e(DMA) = 115 000).[40,41] The stresses at the early stage of the tensile test (Young modulus) of the A_xBA_x block–graft copolymers (dashed and solid lines) were apparently dependent on the PSt content and were much higher than those of the corresponding ABA copolymers (dotted and dashed–dotted lines). We also ascribe these differences to the differences in the morphologies. The tensile strength and strain at break of the A_xBA_x block–graft copolymers were comparable to those of the corresponding ABA samples. In contrast, the values of tensile strength and strain at break for multigraft copolymers with equally spaced graft chains prepared by living anionic polymerization increased in proportion to the number of the junction points.[6] Thus, the mechanical properties at break for these DMA/St copolymers are dependent on the comonomer content but not on the microphase structure, whereas the dynamic viscoelasticity and the Young modulus are determined by the morphology. These results suggest that the A_xBA_x block–graft copolymers have specific mechanical properties, which are clearly different from those of the ABA triblock copolymers and graft copolymers with equally spaced graft chains. The rheological properties of the A_xBA_x block–graft copolymers are now under investigation.

Conclusions

Novel well-defined A_xBA_x-type block–graft copolymers were prepared readily by ruthenium-catalyzed living radical block and graft copolymerization. The characteristic nanoordered microphase separation, which is different from that of conventional ABA triblock copolymers, resulted in different types of TPEs. This study widens the scope of materials design based on well-defined copolymer structures, as the morphologies of these copolymers can be controlled by changing the molecular architecture, that is, the branching number, without changing the comonomer composition, which may affect other properties of the material.

Experimental Section

Materials

Styrene (Wako Chemicals, >98%), DMA (Tokyo Kasei, >99%), and TMSHEMA (Aldrich, >96%) were distilled from calcium hydride under reduced pressure before use. $[Ru(Ind)Cl(PPh_3)_2]$ and $[Ru(Cp^*)Cl(PPh_3)_2]$ (both provided by Wako Chemicals) were used as received. All metal compounds were handled in a glove box (VAC Nexus) under a moisture- and oxygen-free argon atmosphere (<1 ppm O_2). Toluene was distilled over sodium benzophenone ketyl, and dry nitrogen was bubbled into it for 15 min just before use. nBu$_3$N (an additive) and tetralin (an internal standard for NMR spectroscopic or gas chromatographic analysis of the monomers) were distilled from calcium hydride before use. 2-Bromoiso-

Table 2. Tensile properties of A_xBA_x block–graft and ABA triblock copolymers.

Code[a]	F[b] (m+2)	DMA/St (w/w)[b]	Young modulus [MPa]	100% modulus [MPa]	Tensile strength at break [MPa]	Elongation at break [%]	Morphology[c]
4	10.9	82:18	8.4	1.6	1.8	310	cylinders
7	10.9	70:30	210	–	5.6	66	lamellae
11	2	81:19	0.33	0.18	1.3	280	spheres
12	2	70:30	3.5	3.3	4.6	140	cylinders

[a] Code numbers as in Table 1. [b] Determined by ^{1}H NMR spectroscopy. [c] Observed by transmission electron microscopy (TEM).

butyryl bromide (Aldrich, >98%) and 2,2-dichloroacetophenone (Aldrich, >97%) were distilled before use.

Synthesis of the Multifunctional Macroinitiator

All polymerizations were carried out by syringe techniques under dry nitrogen in a flask equipped with a three-way stopcock.

Typical procedure: $[Ru(Ind)Cl(PPh_3)_2]$ (25.4 mg, 0.032 mmol), toluene (14.3 mL), tetralin (0.5 mL), DMA (46.8 mL, 160 mmol), $CHCl_2(COPh)$ (0.8 mL of a 400 mM solution in toluene, 0.320 mmol), and nBu_3N (1.6 mL of a 400 mM solution in toluene, 0.640 mmol) were placed in a 100-mL round-bottomed flask at room temperature. (The total volume of the reaction mixture was 64.0 mL.) The flask was placed in an oil bath maintained at 80°C, and the reaction mixture was stirred vigorously. When the monomer conversion had reached 93% (46 h), TMSHEMA (3.2 mL of a 1.0 M solution in toluene, 3.20 mmol) was added. After a predetermined period of time (38 h), the polymerization was terminated by cooling the reaction mixture to −78°C. Monomer conversion was determined by ^{1}H NMR spectroscopy with tetralin as an internal standard. Toluene (20 mL) and 2-bromoisobutyryl bromide (0.8 mL, 6.4 mmol, 2.0 equiv with respect to the trimethylsilyoxy units) were added to the quenched reaction mixture, and the resulting mixture was stirred at room temperature for 24 h then precipitated into acetone. The precipitate was then dissolved in toluene and reprecipitated in acetone. This precipitation was repeated twice. The precipitate was then dissolved in toluene and reprecipitated into methanol. This procedure was repeated three times. The precipitate was then evaporated to dryness and dried overnight in vacuo at room temperature to yield the product (38.0 g, 93%; M_n = 97000, M_w/M_n = 1.17). The polymer was dissolved in distilled toluene to give a 2.0 M solution for graft copolymerization.

Synthesis of A_xBA_x Block–Graft Copolymers

Graft copolymerizations were also carried out by syringe techniques under dry nitrogen in a flask equipped with a three-way stopcock.

Typical procedure: The macroinitiator I_xBI_x (17.7 mL, 0.381 mmol with respect to the C−Br bonds), toluene (5.0 mL), tetralin (1.7 mL), styrene (13.5 mL, 117 mmol), $[Ru(Ind)Cl(PPh_3)_2]$ (30 mg, 0.038 mmol), and nBu_3N (0.48 mL of a 400 mM solution in toluene, 0.192 mmol) were placed in a 50-mL round-bottomed flask at room temperature. (The total volume of the reaction mixture was 38.4 mL.) The flask was placed in an oil bath maintained at 100°C, and the reaction mixture was stirred vigorously. After a predetermined period of time, the polymerization was terminated by cooling the reaction mixture to −78°C. Monomer conversion was determined by gas chromatography with hexane as an internal standard. The quenched reaction mixture was precipitated into methanol, and the precipitate was isolated by centrifugation. The precipitation was repeated twice, then the precipitate was evaporated to dryness and dried overnight in vacuo at room temperature to yield the product (6.36 g, 94%; M_n = 136000, M_w/M_n = 1.22).

Synthesis of ABA Triblock Copolymers by Ruthenium-Catalyzed Block Copolymerization of Styrene

Typical procedure for the synthesis of the poly(DMA) bifunctional macroinitiator: $[Ru(Ind)Cl(PPh_3)_2]$ (12.7 mg, 0.017 mmol), toluene (7.0 mL), tetralin (0.6 mL), DMA (23.4 mL, 79.8 mmol), $CHCl_2(COPh)$ (0.1 mL of a 800 mM solution in toluene, 0.080 mmol), and nBu_3N (0.80 mL of 400 mM solution in toluene, 0.320 mmol) were placed in a 50-mL round-bottomed flask at room temperature. (The total volume of the reaction mixture was 32.0 mL.) The flask was placed in an oil bath maintained at 80°C, and the reaction mixture was stirred vigorously. After a predetermined period of time (10 h), the polymerization was terminated (at ≈56% conversion) by cooling the reaction mixture to −78°C. Monomer conversion was determined by ^{1}H NMR spectroscopy with tetralin as an internal standard. The reaction mixture was precipitated into acetone, and the precipitate was isolated by centrifugation. The precipitation was repeated twice. The precipitate was then dissolved in toluene and precipitated into methanol. This procedure was repeated three times. The precipitate was then evaporated to dryness and dried overnight in vacuo at room temperature to yield the product (12.5 g, 94%; M_n = 123000, M_w/M_n = 1.18). The polymer was dissolved in distilled toluene to give a 2.0 M solution for block copolymerization.

Typical procedure for the block copolymerization of styrene: The poly(DMA) bifunctional macroinitiator (18.2 mL, 0.0702 mmol with respect to the C−Cl bonds), tetralin (0.50 mL), styrene (6.5 mL, 56.5 mmol), $[Ru(Cp^*)Cl(PPh_3)_2]$ (89.5 mg, 0.112 mmol), and nBu_3N (2.81 mL of a 400 mM solution in toluene, 1.12 mmol) were placed in a 50-mL round-bottomed flask at room temperature. (The total volume of the reaction mixture was 28.1 mL.) The flask was placed in an oil bath maintained at 80°C, and the reaction mixture was stirred vigorously. After a predetermined period of time, the polymerization was terminated by cooling the reaction mixture to −78°C. Monomer conversion was determined by gas chromatography with tetralin as an internal standard. The quenched reaction mixture was precipitated into acetone, and the precipitate was isolated by centrifugation. The precipitation was repeated twice, then the precipitate was evaporated to dryness and dried overnight in vacuo at room temperature to yield the product (6.65 g, 93%; M_n = 214000, M_w/M_n = 1.20).

Detachment of PSt Graft Chains from the Backbone

The A_xBA_x block–graft copolymer with PSt graft chains (50 mg) was placed in a 25-mL round-bottomed flask and dissolved in *N*,*N*-dimethylformamide (7.5 mL). A solution of KOH (0.3 g) in methanol (2.5 mL) was added, and the mixture was heated at 60°C for 24 h. The solvent was then removed by evaporation, and $CHCl_3$ (10.0 mL) was added to the remaining solid. The resulting solution was washed with water (3× 10.0 mL), and the organic layer was evaporated to dryness to yield the product, which was subsequently dried overnight in vacuo at room temperature to give 39 mg of a mixture of the backbone polymers and the detached PSt.

Measurements

^{1}H NMR spectra were recorded on a Varian Gemini 2000 spectrometer (400 MHz). The number-average molecular weights (M_n) and molecular-weight distributions (MWDs: M_w/M_n) of the polymers were measured by SEC with THF at a flow rate of 1.0 mL min^{-1} at 40°C on two polystyrene-gel Shodex KF-805L columns connected to a JASCO PU-980 precision pump and a JASCO RI-930 detector. The molecular weight was calibrated against seven standard poly(methyl methacrylate) samples (M_n = 1,990–6,590,000) or eight standard polystyrene samples (M_n = 526–900,000). Monomer conversions were determined from the concentration of the residual monomer as measured by gas chromatography with tetralin as an internal standard. The absolute weight-average molecular weight (M_w) of the polymers was determined by multiangle laser light scattering in tetrahydrofuran (THF) at 40°C on a Wyatt Technology DAWN DSP photometer (λ = 633 nm). The refractive index increment (d*n*/d*c*) was measured in THF at 25°C on a Wyatt Optilab rEX refractometer (λ = 633 nm); the d*n*/d*c* values were in the range 0.072–0.160 mL g^{-1} for the A_xBA_x block–graft copolymers. The glass transition temperature (T_g) of the polymers was recorded by differential scanning calorimetry on an SSC-5200 instrument (Seiko Instruments Inc.). Samples were first heated to 150°C at 10°C min^{-1}, then equilibrated at this temperature for 5 min, and cooled to −120°C at 5°C min^{-1}. The samples were held at this temperature for 20 min, then reheated to 150°C at 10°C min^{-1}. All T_g values were obtained from the second scan after removing the thermal history. Sample films for dynamic tensile viscoelasticity were prepared by hot-press molding of the copolymers at 230°C. Dynamic tensile storage (E') and loss (E'') moduli and tan δ (E''/E') were measured on a UBM Rheogel-E4000 spectrometer operating at a frequency of 11 Hz (heating rate: 10°C min^{-1}). For TEM, a film specimen was prepared by casting from a 5 wt% solution in toluene for 2 weeks. The cast film was annealed at 140°C for 24 h under vacuum and stained subsequently by exposure to ruthenium tetraoxide (RuO_4) vapor for 2 min. The stained film thus obtained was cryomicrotomed with a diamond knife at −120°C by using a Lica Ultracut UCT. The ultrathin section of approximately 100 nm was transferred onto a Cu mesh grid with a polyvinylformal substrate. TEM and TEMT experiments were performed with an energy-filtering transmission electron microscope with a field-

emission gun operated at 200 kV (JEM-2200FS, JEOL Co., Ltd., Japan).[31a] The tensile properties (Young modulus, tensile strength at break, and elongation at break) were measured on compression-molded dogbone specimens (width: ≈4.0 mm; thickness: ≈0.6–0.7 mm) by using an Instron Universal Testing Machine 5566 at a crosshead speed of 200 mm min^{-1} at 23 °C. At least two specimens per sample were tested.

Acknowledgements

This research was supported in part by the 21st Century COE Program "Nature-Guided Materials Processing", the Ogasawara Foundation for the Promotion of Science and Engineering, the Iketani Science and Technology Foundation, the Izumi Science and Technology Foundation, and the Project to Develop "Innovative Seeds" of the Japan Science and Technology Agency. H.J. is grateful to the New Energy and Industrial Technology Development Organization (NEDO) for supporting this study through the Japanese National Project "Nano Structure Polymer Project" of the Ministry of Economy, Trade, and Industry. H.J. also thanks the Japan Society for the Promotion of Science for partial support of this research through a Grant-in-Aid for Scientific Research (C) (No. 18550194). We thank Atsuhiro Nakahara, Katsuei Takahashi, and Isamu Okamoto (Kuraray Co. Ltd, Tsukuba Research Laboratories) for the measurements of tensile viscoelasticity and tensile tests.

[1] a) G. Riess, G. Hurtrez, P. Bahadur in *Block Copolymers*: *Encyclopedia of Polymer Science and Engineering*, *Vol. 2*, *2nd ed.*, Wiley, New York, **1985**, pp. 324–434; b) F. S. Bates, G. H. Fredrickson, *Annu. Rev. Phys. Chem.* **1990**, *41*, 525–557; c) F. S. Bates, G. H. Fredrickson, *Phys. Today* **1999**, *52*, 32–38; d) V. Avetz, P. F. W. Simon, *Adv. Polym. Sci.* **2005**, *189*, 125–212.

[2] a) *Block Copolymers in Nanoscience* (Eds.: M. Lazzari, G. Liu, S. Lecommandoux), Wiley-VCH, Weinheim, **2006**; b) C. J. Hawker, K. Wooley, *Science* **2005**, *309*, 1200–1205; c) C. J. Hawker, T. P. Russell, *MRS Bull.* **2005**, *30*, 952–967; d) K. Naito, H. Hieda, M. Sakurai, Y. Kamata, K. Asakawa, *IEEE Trans. Magn.* **2002**, *38*, 1949–1951.

[3] G. Holden, H. R. Kricheldorf, R. P. Quirk, *Thermoplastic Elastomers*, *3rd ed.*, Hanser Publishers, Munich, **2004**.

[4] a) M. Morton, *Anionic Polymerization*: *Principles and Practice*, Academic Press, New York, **1983**, pp. 221–232; b) J. P. Kennedy, B. Ivan, *Designed Polymers by Carbocationic Macromolecular Engineering: Theory and Practice*, Hanser Publishers, Munich, **1992**, p. 96; c) M. Sawamoto, M. Kamigaito in *New Methods of Polymer Synthesis*, *Vol. 2* (Eds.: J. R. Ebdon, G. C. Eastmond), Blackie, Glasgow, **1995**, pp. 37–68.

[5] a) M. Xenidou, F. L. Beyer, N. Hadjichristidis, S. P. Gido, N. B. Tan, *Macromolecules* **1998**, *31*, 7959–7967; b) F. L. Beyer, S. P. Gido, C. Büschl, H. Iatrou, D. Uhrig, J. W. Mays, M. Y. Chang, B. A. Garetz, N. P. Balsara, N. B. Tan, N. Hadjichristidis, *Macromolecules* **2000**, *33*, 2039–2048.

[6] a) R. Weidisch, S. P. Gido, D. Uhrig, H. Iatrou, J. W. Mays, N. Hadjichristidis, *Macromolecules* **2001**, *34*, 6333–6337; b) Y. Zhu, R. Weidisch, S. P. Gido, G. Veils, N. Hadjichristidis, *Macromolecules* **2002**, *35*, 5903–5909; c) D. Uhrig, J. W. Mays, *Macromolecules* **2002**, *35*, 7182–7190; d) Y. Zhu, E. Burgaz, S. P. Gido, U. Staudinger, R. Weidisch, D. Uhrig, J. W. Mays, *Macromolecules* **2006**, *39*, 4428–4436.

[7] a) D. J. Pochan, S. P. Gido, S. Pispas, J. W. Mays, A. J. Ryan, J. P. A. Fairclough, I. W. Hamley, N. J. Terrill, *Macromolecules* **1996**, *29*, 5091–5098; b) Y. Tselikas, H. Iatrou, N. Hadjichristidis, K. S. Liang, K. Mohanty, D. J. Lohse, *J. Chem. Phys.* **1996**, *105*, 2456–2462; c) F. L. Beyer, S. P. Gido, G. Veils, N. Hadjichristidis, N. B. Tan, *Macromolecules* **1999**, *32*, 6604–6607; d) L. Yang, S. Hong, S. P. Gido, G. Veils, N. Hadjichristidis, *Macromolecules* **2001**, *34*, 9069–9073.

[8] a) A. Mavroudis, A. Avgeropoulos, N. Hadjichristidis, E. L. Thomas, D. J. Lohse, *Chem. Mater.* **2003**, *15*, 1976–1983; b) A. Mavroudis, A. Avgeropoulos, N. Hadjichristidis, E. L. Thomas, D. J. Lohse, *Chem. Mater.* **2006**, *18*, 2164–2168.

[9] a) Y. Matsushita, J. Watanabe, F. Katano, Y. Yoshida, I. Noda, *Polymer*, **1996**, *2*, 321–325; b) Y. Matsushita, *J. Polym. Sci. Part B*: *Polym. Phys.* **2000**, *38*, 1645–1655.

[10] a) S. P. Gido, C. Lee, D. J. Pochan, S. Pispas, J. W. Mays, N. Hadjichristidis, *Macromolecules* **1996**, *29*, 7022–7028; b) C. Lee, S. P. Gido, Y. Poulos, N. Hadjichristidis, N. B. Tan, S. F. Trevino, J. W. Mays, *J. Chem. Phys.* **1997**, *107*, 6460–6469.

[11] For the synthesis of polymers of the type A_xBA_x, see: a) S. Houli, H. Iatrou, N. Hadjichristidis, D. Vlassopoulos, *Macromolecules* **2002**, *35*, 6592–6597; b) D. M. Knauss, T. Huang, *Macromolecules* **2002**, *35*, 2055–2062; c) T. Huang, D. M. Knauss, *Polym. Bull.* **2002**, *58*, 143–150; d) T. Huang, D. M. Knauss, *Macromol. Symp.* **2004**, *215*, 81–93; e) M.-K. Lai, J.-Y. Wang, R. C.-C. Tsiang, *Polymer* **2005**, *46*, 2558–2566.

[12] a) M. K. Georges, R. P. N. Veregin, P. M. Kazmaier, G. K. Hamer, *Macromolecules* **1993**, *26*, 2987–2988; b) M. K. Georges, R. P. N. Veregin, P. M. Kazmaier, G. K. Hamer, *Trends Polym. Sci.* **1994**, *2*, 66–72.

[13] a) C. J. Hawker, *J. Am. Chem. Soc.* **1994**, *116*, 11185–11186; b) C. J. Hawker, A. W. Bosman, E. Harth, *Chem. Rev.* **2001**, *101*, 3661–3688.

[14] a) M. Kato, M. Kamigaito, M. Sawamoto, T. Higashimura, *Macromolecules* **1995**, *28*, 1721–1723; b) M. Kamigaito, T. Ando, M. Sawamoto, *Chem. Rev.* **2001**, *101*, 3689–3745; c) M. Kamigaito, T. Ando, M. Sawamoto, *Chem. Rec.* **2004**, *4*, 159–175.

[15] a) J.-S. Wang, K. Matyjaszewski, *J. Am. Chem. Soc.* **1995**, *117*, 5614–5615; b) K. Matyjaszewski, J. Xia, *Chem. Rev.* **2001**, *101*, 2921–2990.

[16] a) J. Chiefari, Y. K. Chong, F. Ercole, J. Krstina, K. Jeffery, T. P. T. Le, R. T. A. Mayadunne, G. F. Meijs, C. L. Moad, G. Moad, E. Rizzardo, S. H. Thang, *Macromolecules* **1998**, *31*, 5559–5562; b) G. Moad, E. Rizzardo, S. H. Thang, *Aust. J. Chem.* **2005**, *58*, 379–410.

[17] M. Destarac, W. Bzducha, D. Taton, I. Gauthier-Gillaizeau, S. Z. Zard, *Macromol. Rapid Commun.* **2002**, *23*, 1049–1054.

[18] For reviews, see: a) K. A. Davis, K. Matyjaszewski, *Adv. Polym. Sci.* **2002**, *159*, 107–152; b) H. G. Börner, K. Matyjaszewski, *Macromol. Symp.* **2002**, *177*, 1–15; c) A. Bhattacharya, B. N. Misra, *Prog. Polym. Sci.* **2004**, *29*, 767–814.

[19] a) K. L. Beers, S. G. Gaynor, K. Matyjaszewski, S. S. Sheiko, M. Möller, *Macromolecules* **1998**, *31*, 9413–9415; b) H. G. Börner, K. L. Beers, K. Matyjaszewski, S. S. Sheiko, M. Möller, *Macromolecules* **2001**, *34*, 4375–4383; c) H. G. Börner, D. Duran, K. Matyjaszewski, M. da Silva, S. S. Sheiko, *Macromolecules* **2002**, *35*, 3387–3394; d) S. Qin, K. Matyjaszewski, H. Xu, S. S. Sheiko, *Macromolecules* **2003**, *36*, 605–612; e) S. J. Lord, S. S. Sheiko, I. LaRue, H.-I. Lee, K. Matyjaszewski, *Macromolecules* **2004**, *37*, 4235–4240; f) H. Lee, K. Matyjaszewski, S. Yu, S. S. Sheiko, *Macromolecules* **2005**, *38*, 8264–8271.

[20] a) G. Cheng, A. Böker, M. Zhang, G. Krausch, A. H. E. Müller, *Macromolecules* **2001**, *34*, 6883–6888; b) H. Mori, A. H. E. Müller, *Prog. Polym. Sci.* **2003**, *28*, 1403–1439; c) Y. Cai, M. Hartenstein, A. H. E. Müller, *Macromolecules* **2004**, *37*, 7484–7490.

[21] Y. Miura, K. Satoh, M. Kamigaito, Y. Okamoto, *Polym. J.* **2006**, *38*, 930–939.

[22] For the synthesis of a macrocyclic graft copolymer, see: Z. Jia, Q. Fu, J. Huang, *Macromolecules* **2006**, *39*, 5190–5193.

[23] a) E. Ruckenstein, H. Zhang, *Macromolecules* **1998**, *31*, 2977–2982; b) H. Zhang, E. Ruckenstein, *Macromolecules* **1998**, *31*, 4753–4759.

[24] F. Lecolley, C. Waterson, A. J. Carmichael, G. Mantovani, S. Harrisson, H. Chappell, A. Limer, P. Williams, K. Ohno, D. M. Haddleton, *J. Mater. Chem.* **2003**, *13*, 2689–2695.

[25] S. Ohno, K. Matyjaszewski, *J. Polym. Sci. Part A*: *Polym. Chem.* **2006**, *44*, 5454–5467.

[26] a) Q. Pan, S. Liu, J. Xie, M. Jiang, *J. Polym. Sci. Part A*: *Polym. Chem.* **1999**, *37*, 2699–2702; b) F. Ning, M. Jiang, M. Mu, H. Duan, J. Xie, *J. Polym. Sci. Part A*: *Polym. Chem.* **2002**, *40*, 1253–1266.

[27] a) J. H. Truelsen, J. Kops, W. Batsberg, *Macromol. Rapid Commun.* **2000**, *21*, 98–102; b) J. H. Truelsen, J. Kops, W. Batsberg, S. P. Armes, *Macromol. Chem. Phys.* **2002**, *203*, 2124–2131; c) J. H. Truel-

sen, J. Kops, W. Batsberg, S. P. Armes, *Polym. Bull.* **2002**, *58*, 235–242.
[28] a) Y. G. Li, P. J. Shi, C. Y. Pan, *Macromolecules* **2004**, *37*, 5190–5195; b) Y. Cong, B. Y. Li, Y. C. Han, Y. G. Li, C. Y. Pan, *Macromolecules* **2005**, *38*, 9836–9846.
[29] T. Pakula, Y. Zhang, K. Matyjaszewski, H. Lee, H. Börner, S. Qin, G. C. Berry, *Polymer* **2006**, *47*, 7198–7206.
[30] Y. Miura, K. Satoh, M. Kamigaito, Y. Okamoto, T. Kaneko, H. Jinnai, S. Kobukata, *Macromolecules* **2007**, *40*, 465–473.
[31] a) H. Jinnai, Y. Nishikawa, T. Ikehara, T. Nishi, *Adv. Polym. Sci.* **2004**, *170*, 115–167; b) N. Kawase, M. Kato, H. Nishioka, H. Jinnai, *Ultramicroscopy* **2007**, *107*, 8–15; c) H. Nishioka, K. Niihara, T. Kaneko, J. Yamanaka, Y. Nishikawa, T. Inoue, T. Nishi, H. Jinnai, *Compos. Interfaces.* **2006**, *13*, 589–603; d) H. Sugimori, T. Nishi, H. Jinnai, *Macromolecules* **2005**, *38*, 10226–10233; e) T. Kaneko, H. Nishioka, Y. Nishikawa, T. Nishi, H. Jinnai, *J. Electron. Micros.* **2005**, *54*, 437–444.
[32] a) T. Kaneko, K. Suda, K. Satoh, M. Kamigaito, T. Kato, T. Ono, E. Nakamura, T. Nishi, H. Jinnai, *Macromol. Symp.* **2006**, *242*, 80–86; b) H. Jinnai, T. Kaneko, H. Nishioka, H. Hasegawa, T. Nishi, *Chem. Rec.* **2006**, *6*, 267–274; c) H. Jinnai, H. Hasegawa, Y. Nishikawa, G. J. A. Sevink, M. B. Braunfeld, D. A. Agard, R. J. Spontak, *Macromol. Rapid Commun.* **2006**, *27*, 1424–1429; d) H. Jinnai, K. Sawa, T. Nishi, *Macromolecules* **2006**, *39*, 5815–5819.
[33] S. S. Rogers, L. Mandelkern, *J. Phys. Chem.* **1957**, *61*, 985–990.
[34] *Polymer Handbook*, *4th ed.* (Eds.: J. Brandrup, E. H. Immergut, E. A. Grulke), Wiley-Interscience, New York, **1999**, V/93.
[35] B. S. Sumerlin, D. Neugebauer, K. Matyjaszewski, *Macromolecules* **2005**, *38*, 702–708.
[36] S. T. Milner, *Macromolecules* **1994**, *27*, 2333–2335.
[37] S. P. Gido, D. W. Schwark, E. L. Thomas, M. C. Gonçalves, *Macromolecules* **1993**, *26*, 2636–2640.
[38] H. Hückstädt, A. Göpfert, V. Abetz, *Macromol. Chem. Phys.* **2000**, *201*, 296–307.
[39] K. Takahashi, H. Hasegawa, T. Hashimoto, V. Bellas, H. Iatrou, N. Hadjichristidis, *Macromolecules* **2002**, *35*, 4859–4861.
[40] L. J. Fetters, D. J. Lohse, W. W. Grassley, *J. Polym. Sci. Part B: Polym. Phys.* **1999**, *37*, 1023–1033.
[41] J.-D. Tong, R. Jérôme, *Macromolecules* **2000**, *33*, 1479–1481.

Received: December 5, 2006
Revised: February 6, 2007

